Stability evaluation of anterior external fixation in patient with unstable pelvic ring fracture: a finite element analysis

Lan Li[1,2#], Jingwei Lu[3#], Longfei Yang[1], Kaijia Zhang[2], Jing Jin[2], Guojing Sun[3], Xingsong Wang[1], Qing Jiang[2]

[1]School of Mechanical Engineering, Southeast University, Nanjing 211189, China; [2]State Key Laboratory of Pharmaceutical Biotechnology, Department of Sports Medicine and Adult Reconstructive Surgery, Drum Tower Hospital Affiliated to Medical School of Nanjing University, Nanjing 210008, China; [3]Department of Orthopedics, Nanjing Jinling Hospital, Nanjing 210093, China

Contributions: (I) Conception and design: L Li, J Lu; (II) Administrative support: X Wang, Q Jiang; (III) Provision of study materials or patients: J Lu; (IV) Collection and assembly of data: J Lu, L Yang; (V) Data analysis and interpretation: K Zhang, L Yang, J Jin; (VI) Manuscript writing: All authors; (VII) Final approval of manuscript: All authors.

[#]These authors contributed equally to this work.

Correspondence to: Xingsong Wang, PhD. School of Mechanical Engineering, Southeast University, No. 2 Southeast University Road, Nanjing 211189, China. Email: xswang@seu.edu.cn; Qing Jiang, MD, PhD. Department of Sports Medicine and Adult Reconstructive Surgery, Drum Tower Hospital Affiliated to Medical School of Nanjing University, No. 321 Zhongshan Road, Nanjing 210008, China. Email: qingj@nju.edu.cn.

Background: The pelvic ring fractures (PRF) are commonly induced by the high-energy impact and will lead to unstable and sever injures. This study is aimed to explore the stability of anterior external fixation in treating pelvis fracture and evaluate the possibility for these kinds of patients to reduce bedridden time.

Methods: A patient with Tile B3 pelvis fracture was chosen in the research and the corresponding digital model was reconstructed according to the CT images and 3D scanning. Four angles of pelvis under vertical compression were employed in the finite element (FE) analyses. The stress distribution and micro-motion displacement were calculated to validate the instability of pelvis.

Results: The stress applied on the pelvis was ranged from 4.296 to 8.364 MPa in all postures. The stress applied on pins was less than 7.011 MPa during reclining, and reached 28.29 MPa when standing. The micro-motion displacement in reclining posture was ranged from 0.005 to 0.087 mm. The value increased to more than 1mm in standing posture.

Conclusions: It was safety for patients with pelvis fracture to sit vertical or recline on the bed during nursing or having treatment, but standing or walking will generate inappropriate micro-motion. The existence of external fixation can reduce the possibility of complications caused by long-term bedridden.

Keywords: Pelvic ring fracture (PRF); external fixation; finite element analysis (FE analysis); stability

Introduction

The incidence of pelvic fractures among all fractures can be 4–5%, and the pelvic ring fractures (PRF) account for less than 1% in fractured patients (1). As a kind of PRF, vertical shear (VS.) pelvic fracture, defined as the complete disruption of both anterior and posterior ring, may be induced by falling from a height or a traffic accident and result an unstable situation on pelvic (2). Although the mortality cause by VS. pelvic fractures is lower than PRF, the high-energy impact transmitted axially by the pelvis will lead to instable and sever injures, making stabilization and definitive treatment a complex problem (3). Mechanical pelvic instability accompanied by possible haemodynamic status generally require urgent external fixation for future treatment or rehabilitation therapy. By this way, the vertical

displacement of pelvic can be reduced to decrease the pelvic volume and control haemorrhage. It has been proved that the lack of early fracture reduction may lead to poor functional outcomes, chronic pelvic pain, deformity, and gait disturbance (4). Additionally, the external fixation can improve patients' cardio-respiratory physiology, mobility, and nursing care through an early stabilization with an erect posture (5).

The pelvis of Tile B fractures is unstable in rotation but stable in vertical. This kind of fracture is commonly caused by anterior-posterior trauma or crashing force from lateral direction (6). This situation is usually accompanied by abdominal trauma or gastrointestinal tract injury, which may result in long-term bedridden and cause difficulties for patients' rehabilitation. The most direct impact is the absence of mechanical stress, a vital factor in maintaining bone mass and resisting bone atrophy and osteoporosis (7). In addition, low bone mineral density (BMD), abnormal bone metabolism, and the subsequent fracture are the most serious complications for long period bed confinement (8,9). Besides complications occurred in musculoskeletal system, the pressure ulcer, deep vein thrombosis (DVT), pneumonia, and urinary tract infection (UTI) would happen associated with immobility (10-12). In order to promote bone remolding, recovery gastrointestinal function and reduce complications, helping patients to change their postures under stable condition is necessary.

Herein, we enrolled a patient who suffered from a traffic accident and was diagnosed as severe abdominal injury with Tile B3 PRF. The anterior external fixation was placed at iliac crest with four pins to stable the pelvic ring. To investigate the possibility for reclining or further exercising, finite element (FE) simulation was introduced to calculate the distance and stress of each fragment. In this way, we hoped to find some theoretically proofs to guide the clinical treatment and nursing for these kinds of patients.

Methods

All methods in this study were carried out in accordance with relevant guidelines and regulations. All experimental protocols in this study were approved by the Ethics Committee of Drum Tower Hospital Affiliated to Medical School of Nanjing University.

Data acquisition and 3D reconstruction

A CT scan was performed using a GE Lightspeed 16 CT

equipment (GE, CT, USA) on a female patient with Tile B3 fracture. The lower limb was scanned at the neutral posture with a slice distance of 0.625 mm and a field of view (FOV) of 500 mm. Each part of the external fixation scaffold was scanned by a 3D handheld scanner (EinScan-Pro, Shining 3D, China). A high-definition mode was chosen to complete the scanning process to obtain more accurate images.

The 3D models of the bone structures were reconstructed by MIMICS 19.0 (Materialise, Leuven, Belgium). To minimize the variation in the models, manual segmentation of the bony structures was performed under the supervision of an experienced orthopedist and radiologist with an accuracy of 0.1 mm. The photo of external fixation according to the clinical result and its X-ray image were shown as *Figure 1A,B* respectively. The assembly pelvis and external fixation were shown in *Figure 1C*, in which the fragments of the pelvis were defined as P1 (the left wing of ilium, the sacrum, the coccyx, the left acetabulum, and the left ischial tuberosity), P2 (the right wing of ilium, the right acetabulum, and the right ischial tuberosity), P3 (the right pubic bone and the left inferior pubic ramus), and P4 (the left superior pubic ramus). The fracture line between the fragments were defined from fracture 1 to fracture 6.

FE modeling and material properties

All the data were exported as stereolithography (STL) files, and surface Remesh was operated by Materialise 3-matic 11.0 software. The established models were imported and assembled in Abaqus 2017 (Similia, Rhode Island, USA). The external fixation and the bone, considered as linear materials, were meshed using 4-noded liner tetrahedron (C3D4). For the external fixation, the rods were assumed as carbon fiber, while the pins and the stabilization wrench were assumed as steel. The material behavior was settled based on previous studies (13-15) and the parameters were listed in *Table 1*. To simplify the analysis process, the tibia and other soft tissues, including muscle, ligaments, and skins were not considered in the study.

Loads and boundary conditions

In the present study, the degree was regarded as 0° when the patient was in supine (*Figure 2A*). We included three kinds of angle (30°, 60°, and 90°) in the FE simulation to evaluate the stability of the pelvis ring (*Figure 2B,C,D*). The angle was calculated by the intersection angle between
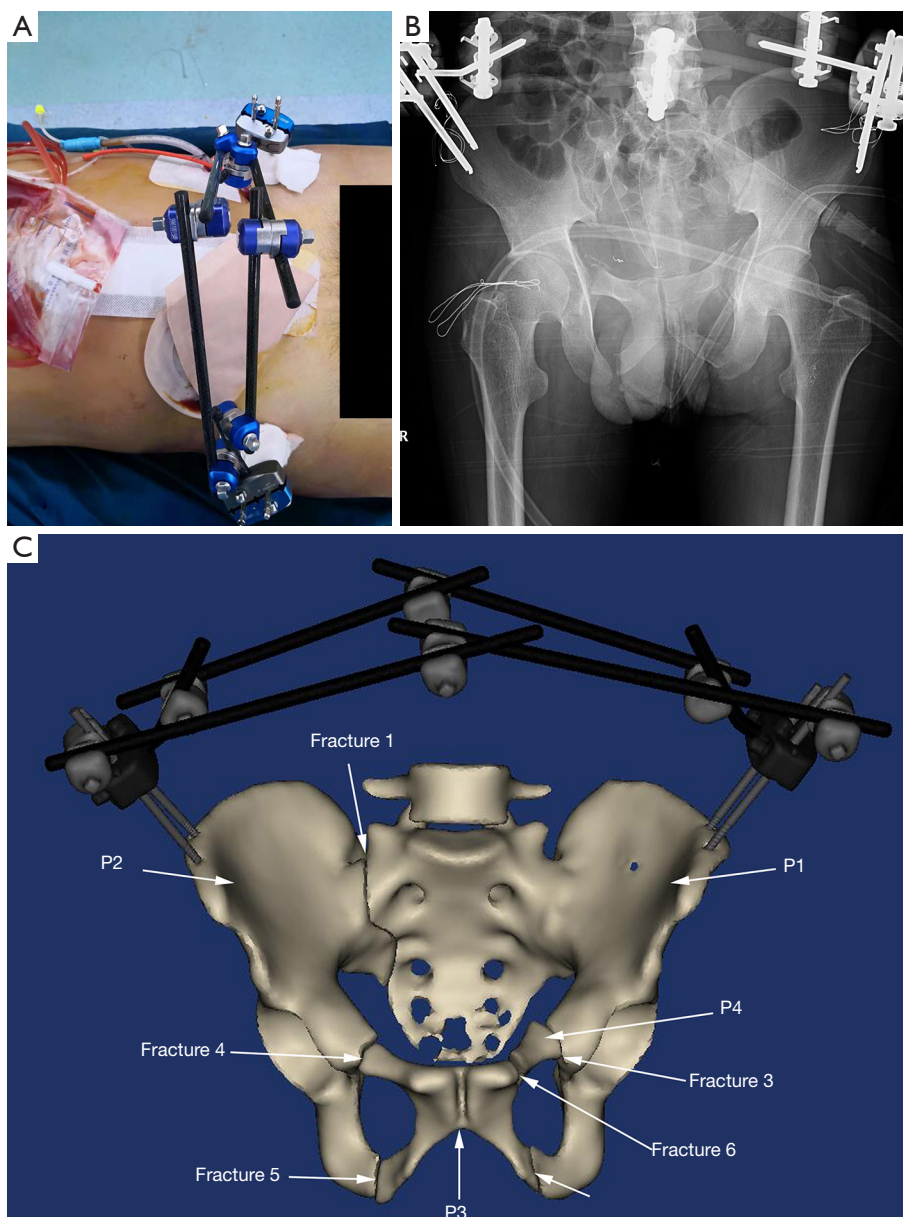
Figure 1 The patients enrolled in the study and the 3D models. (A) The general view of the patient with anterior external fixation; (B) the X-ray of the pelvis; (C) the general view of the pelvis and external fixation digital models used in the FE simulation, the fragments and the fractures line were indicated as the arrows in the figure. FE, finite element.

Table 1 The properties of materials used in FE simulation

Materials	Density (kg/m³)	Young's modulus (GPa)	Yield modulus (MPa)	Possion's ratio
Steel	7,980	200	369	0.31
Carbon fiber	1,760	210	1,916	0.22
Bone	1,700	7.8	85	0.3

Page 4 of 10

Li et al. Stability evaluation for pelvis facture patients using external fixation
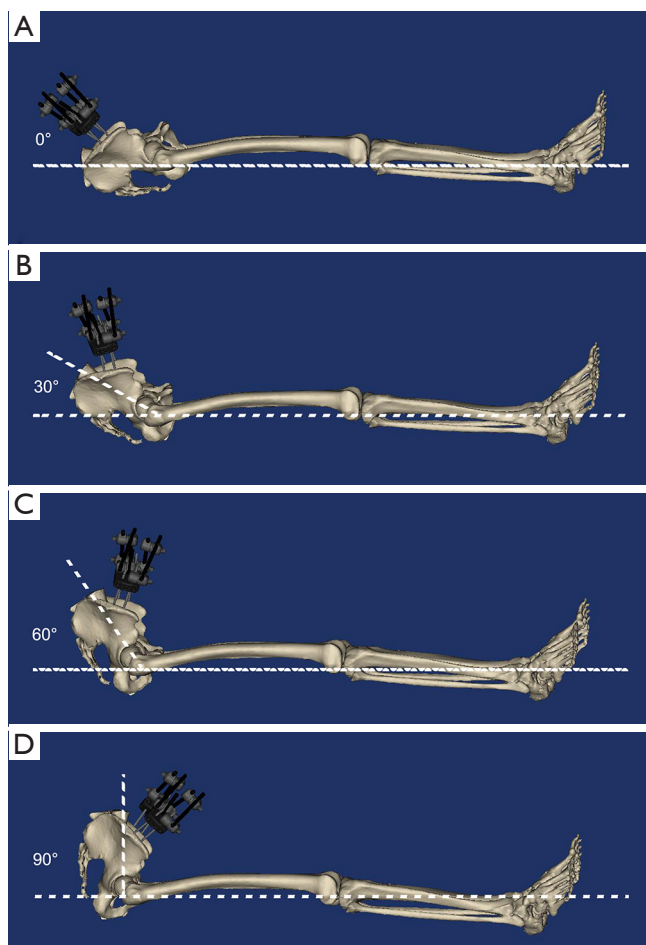
Figure 2 The angles used in the FE simulation. From top to bottom was (A) 0°, (B) 30°, (C) 60°, and (D) 90°, respectively. FE, finite element.

the line from femoral condyle to femoral trochanter and the line from L5 vertebra to femoral trochanter. The threaded surfaces of pins and bones were considered as tie constraints, so as the surfaces between pins and stabilization wrench (16). Frictional contact interactions were assumed between the bones and the friction coefficients was 0.46 (17). A vertical compression load of 350N (half of the body weight) was applied on the vertebral body when the angle was 90°. Considering the change of angle in gravitation, the numerical value of load for 30° and 60° were 175N and 303N, respectively. All nodes on the ischiopubic ramus and femoral condyle were constrained with 0 degrees of freedom to prevent motions during the analysis. In spite of reclining, the standing posture was also simulated at the angle of zero. The same vertical compression load of 350N was applied

on the lumbar vertebra and the femoral condyle, which was fixed in all translational and rotational degrees of freedom.

Results

The stress concentration area on pelvis was changed as the variation of posture. Based on the general view of pelvis (*Figure 3*), we can find that the blue-green region was distributed around the sacroiliac joint and the ischiopubic ramus as the posture was reclining (*Figure 3A,B,C*). But the distribution area was differed, it was obviously that the larger degree demonstrated larger stress area around the sacroiliac joint. For the ischiopubic ramus, the 60° group expressed the largest area. After the posture becomes standing, the blue-green region shifted to the superior pubic ramus, the pubic tubercle, the pubic symphysis, and the sacroiliac joint (*Figure 3D*). Among all the groups, the peak value of stress appeared at the right sacroiliac joint between the fragments P1 and P2, and the numerical value grew as the degree increased (the value was 4.296, 7.326, 8.342, and 8.364 MPa, respectively). The displayed value rises significantly from 30° to 60°, and slightly grows from 60° to 90° until standing.

Unlike bone structures, the stress applied on pins demonstrated notable variation tendency in both numerical value and distribution region. According to the stress nephogram exhibited in *Figure 4A,B,C,D*, the peak value of stress applied on the left pins appeared on the proximal pin. During reclining, the 60° group showed the largest value (7.011 MPa) and area, and the 90° group was slightly larger than the 30° group (4.89 *vs.* 3.793 MPa). The value can reach as high as 25.12 MPa during standing. The same results can be found on the right side (*Figure 4E,F,G,H*), the numerical value in standing posture was the highest (28.29 MPa), followed with the 60° group (5.337 MPa). The 30° group and the 90° group were approximant (2.763 *vs.* 2.527 MPa). However, the peak value appeared on the distal pin.

The variation tendency in displacement of four fragments and the relative movement between each fragment was the same. As we can find in *Figure 5*, the fragments obtained the largest displacement in the 60° group among the reclining postures (ranged from 0.02872 to 0.08673 mm), and the vertical posture gain the smallest displacement (ranged from 0.00521 to 0.03803 mm). The bilateral wing of ilium and the right superior pubic ramus showed a greater degree of displacement, indicating that the P1, P2, and P4 were more unstable. The relative movement
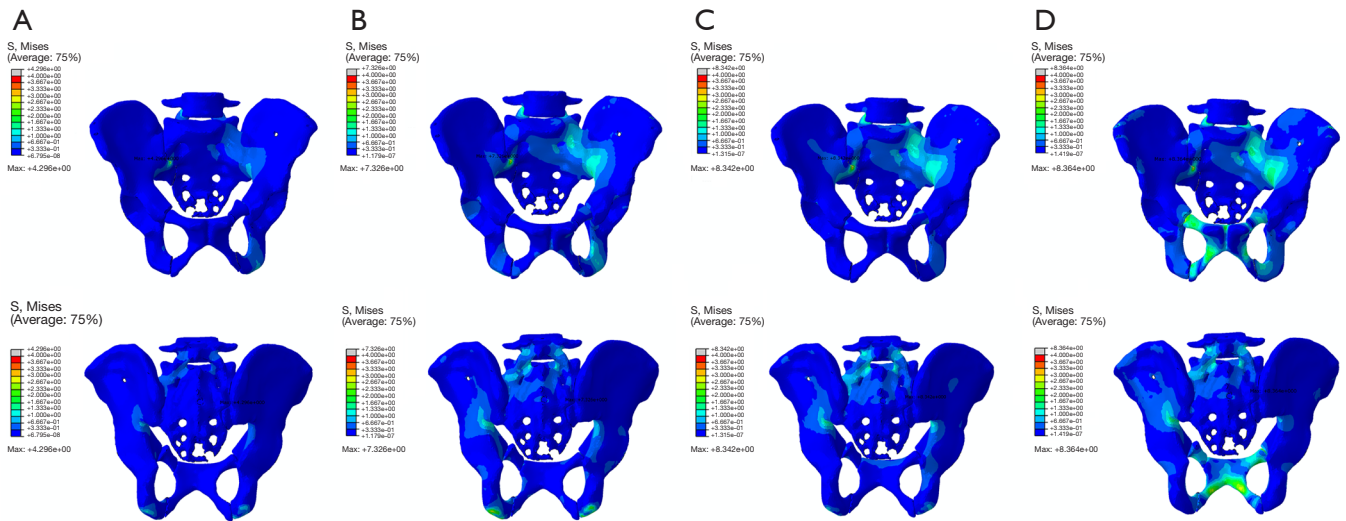
Figure 3 The stress nephogram of the pelvis. The color on the legends changed from red to deep blue that represented the stress variation from large too small. From right side to left side was (A) 0°, (B) 30°, (C) 60°, and (D) 90°, respectively. The front views of the pelvis were placed on the first column and the back views of the pelvis were placed on the second column.
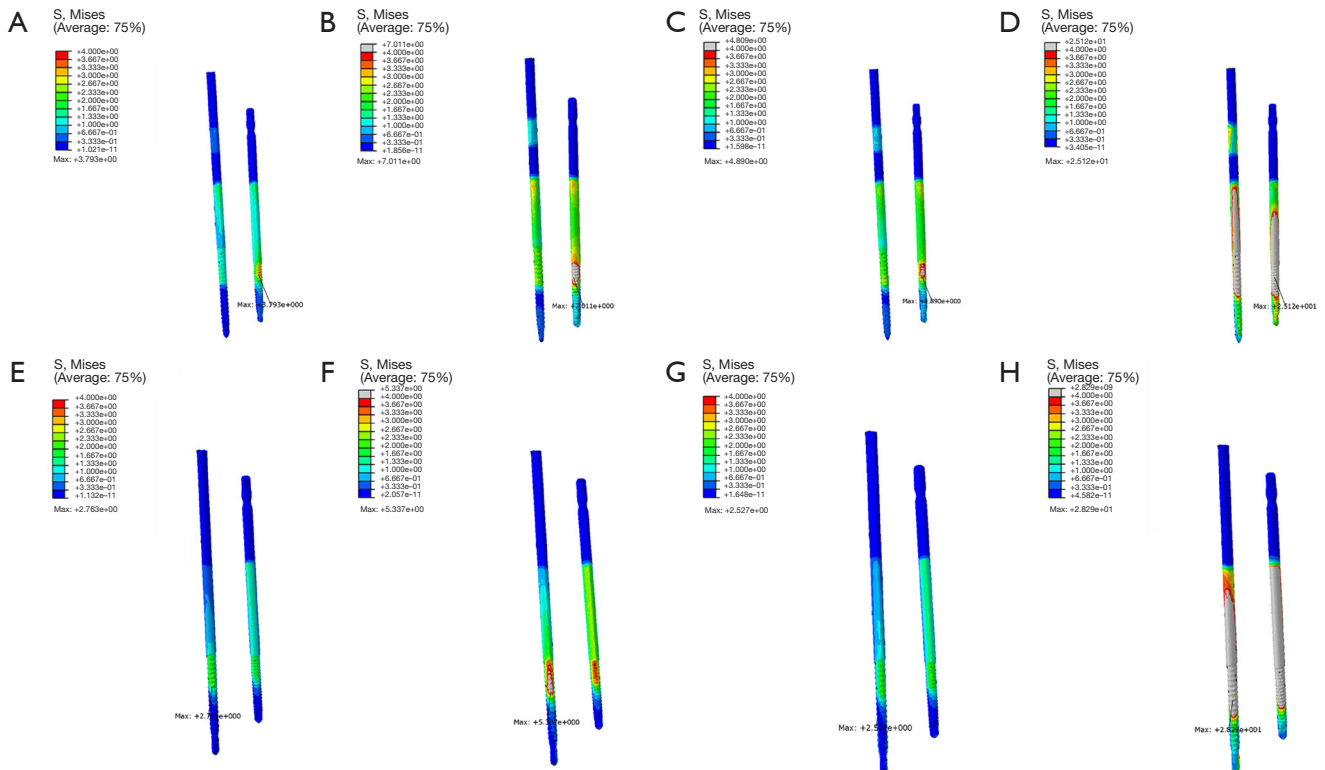
Figure 4 The stress nephogram of the pins. (A) The left pins of 0°; (B) the left pins of 30°; (C) the left pins of 60°; (D) the left pins of 90°; (E) the right pins of 0°; (F) the right pins of 30°; (G) the right pins of 60°; (H) the right pins of 90°.

Page 6 of 10

Li et al. Stability evaluation for pelvis facture patients using external fixation
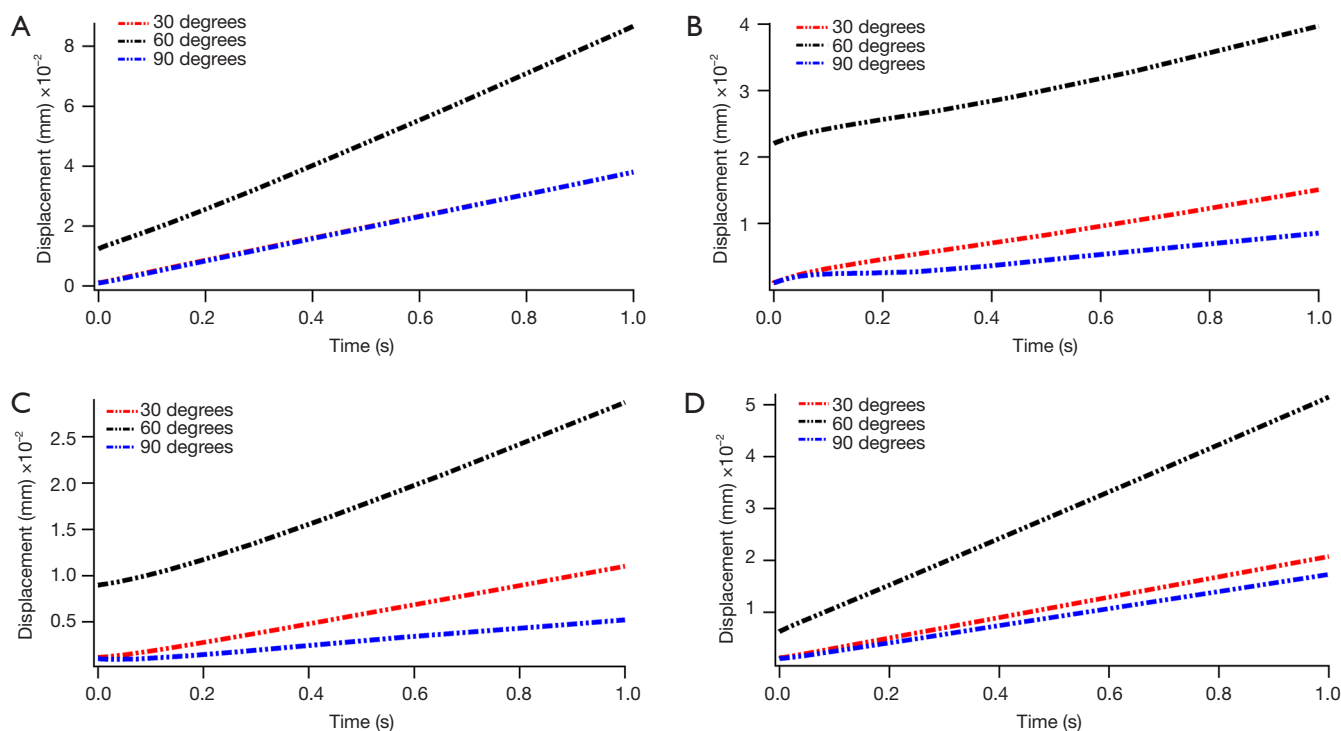
Figure 5 The displacement of each fragment. (A) The displacement of P1; (B) the displacement of P2; (C) the displacement of P3; (D) the displacement of P4.

was correlated with the movement of fragments (*Figure 6*), the larger displacement occurred between the three fragments mentioned above (*Figure 6A,C,F*), the fracture ends around P3 shown smaller relative movement (*Figure 6B,D,E*). However, when standing posture, the movement of the fragments and the relative displacement between them are significantly increased, and the amount of increase can reach two orders of magnitude (*Figure 7*). All the numerical values of displacement exceeded 1 mm under a compression of 50% body weight (ranged from 1.02675 to 1.50127 mm). The fracture end between P1 and P2 showed largest relative movement (1.68501 mm), which was similar to the reclining postures.

Discussion

The mechanical environment plays vital role in osteogenesis, the callus formation can be affected by the interfragmentary movement. In the present study, we analyzed the movement distance of each fragment and the relative movement between fragments under several postures by FE simulation. The results demonstrated that these postures brought slightly displacement between

fracture fragments. According to the previous studies, the motion displacement ranging from 0.1 to 1 mm can improve healing time (18-20). The micro-motion distance in our study was far less than the results in literatures, indicating that the variation of posture will not affect the fracture healing. It is possible and feasible for these patients to sit or do some early rehabilitation exercise.

The FE simulation could reveal the biomechanical environment of pelvis ring better and predict the load transferring and the stress distribution between fixation and bone structures. Based on our results, the pelvis was more stable under vertical posture, meaning that siting on the bed may be better than reclining for fracture healing. This situation was different from the principles of clinical nursing. To verify the interesting result, a simple physical model was introduced in our research. As shown in *Figure 8A*, we employed two mass blocks to simulate the fractured pelvis, and the force in the process of lifting was analyzed. Firstly, the mass block A and B were regarded as a whole system S and the force analysis was carried out. When S was lifted off the horizontal datum level, the system was supported by the reaction force at F_N the fulcrum O and the friction force F_{f_G} in the horizontal
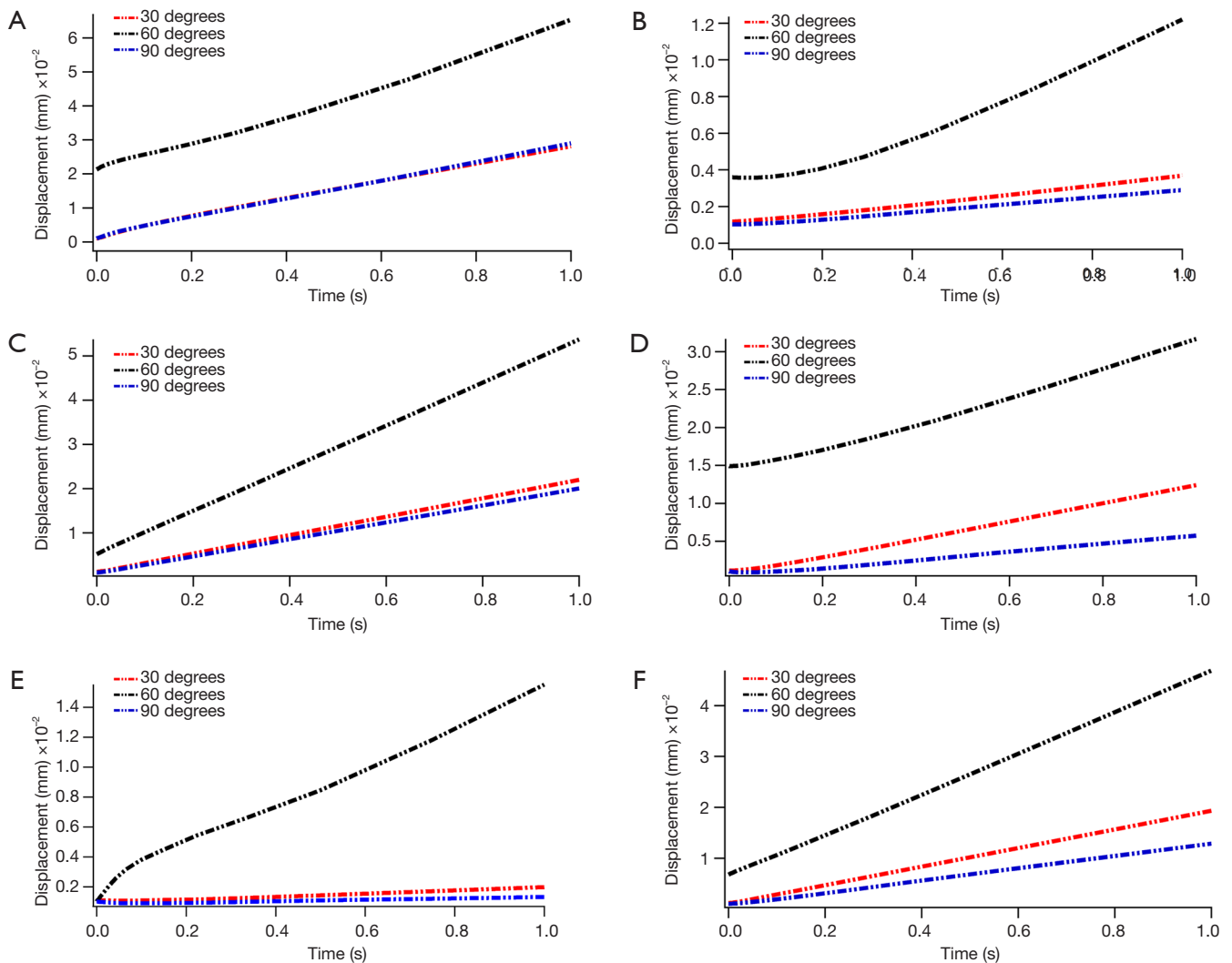
Figure 6 The relative movement between each fragment. (A) The relative movement of fracture 1; (B) the relative movement of fracture 2; (C) the relative movement of fracture 3; (D) the relative movement of fracture 4; (E) the relative movement of fracture 5; (F) the relative movement of fracture 6.
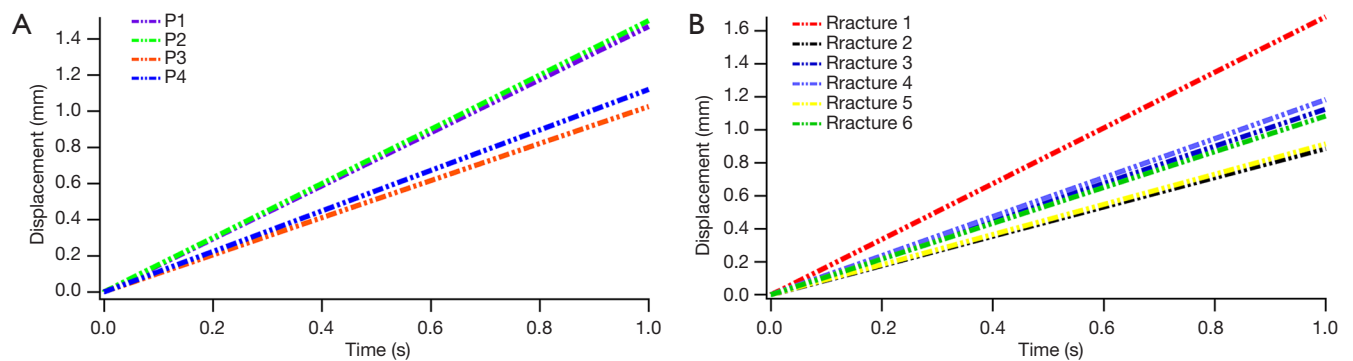
Figure 7 The results of the standing posture. (A) The motion displacement of four fracture fragments; (B) the relative movement of six fracture lines.

Ann Transl Med 2019;7(14):303 | http://dx.doi.org/10.21037/atm.2019.05.65
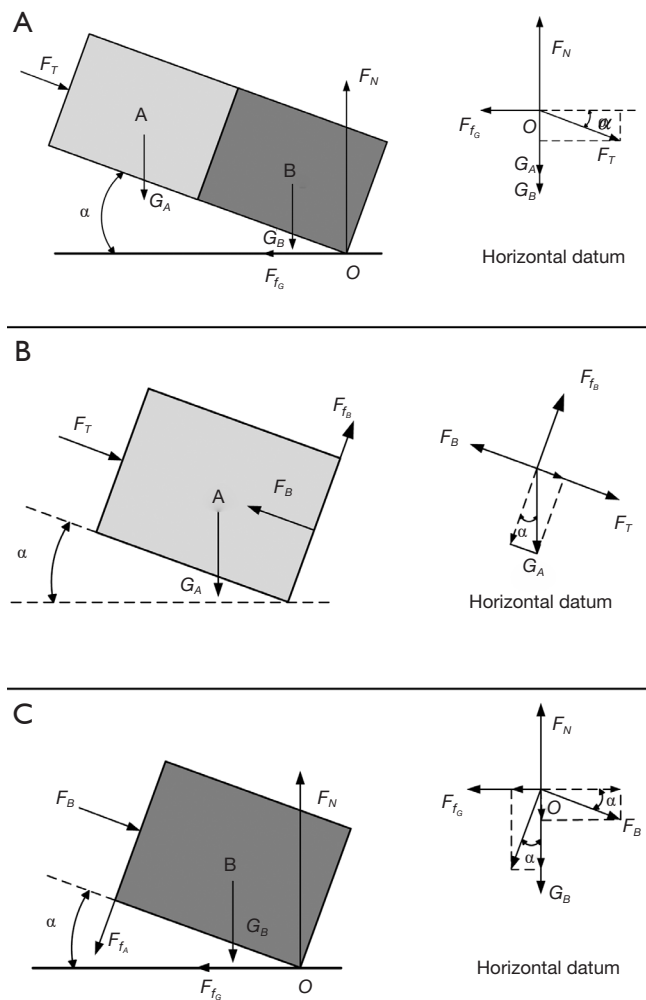
Figure 8 The simplified physical model. (A) Diagram of overall force analysis for system S; (B) diagram of force analysis of mass block A; (C) diagram of force analysis of mass block B.

direction. At the same time, the thrust F_T, the gravity G_A, and the gravity G_B were applied on the system either. According to the equilibrium criterion of force, the external thrust F_T can be decomposed in the horizontal and vertical directions. We can get the equations:

$$F_N = \left(G_A + G_B + F_T \times \sin \alpha \right) \qquad [1]$$

$$F_{f_G} = F_T \times \cos \alpha \qquad [2]$$

Secondly, the mass block A was isolated and analyzed separately (*Figure 8B*). At the interface of two mass blocks, the bottom face of A was subjected to the support force F_A

and the friction force F_{f_B} generated by mass block B. The force G_A can be decomposed along the F_T direction based on the equilibrium criterion of force, and the equation was obtained as follow:

$$F_B = G_A \times \sin \alpha + F_T \qquad [3]$$

Finally, the mass block B was isolated separately and the force analysis was carried out (*Figure 8C*). The top surface of mass block B was subjected to the pressure F_T generated by mass block A and the friction force F_{f_A}. Similarly, we can decompose the F_T and F_{f_A} in the vertical direction to obtain the equilibrium equation:

$$F_B \times \cos \alpha = \left(F_{f_G} + F_{f_A} \times \sin \alpha \right) \qquad [4]$$

The friction force between mass block A and B can be achieved by introducing equation [1], [2], and [3] into equation [4]:

$$F_{f_A} = G_A \times \cos \alpha = m_A g \times \cos \alpha \qquad [5]$$

Due to the constant parameters m_A and g, the friction force was inversely proportional to the lift angle α, indicating that the stability was gradually increased accompanied by the increase of lift angle.

Depending on these foundations, we can conclude that keeping siting or reclining is safety for patients during treating or nursing process. The stress applied on all the fracture in all postures were lower than 10 MPa, which could be considered to strengthen a bone during the remodeling process (21). Furthermore, we explored the possibility for standing, which contributes significantly for the early recovering of gastrointestinal function and mechanical stress applied on bony structures. The results were not optimistic, all the fragments exhibited the motion distance larger than the recommendation in previous literatures. Although the stress applied on the bones and the external fixation were less than the yield modulus during standing, the inadequate micro-motion displacement was not favored for fracture healing.

Several limitations were existed in the study. Firstly, the FE simulations could not precisely reveal the stress variation due to the absence of soft tissues. And the ciomechanical test on human cadaveric pelvis should be conducted further. Second, the entire lifting process cannot be represented by a complete action, but needs to be broken down into different angles. The FE simulation shows the transient response of the pelvic ring under compressive load, and we can only infer the results based on the trend.

Conclusions

We have explored the stress transferring and distribution on the unstable PRF using a realistic digital model. To simulate the lifting process, three representative angles during this process were introduced in the FE simulation. The motion displacement, the stress applied on bony structures, and the stress applied on pins were analyzed. Additionally, the standing posture was also included in the simulation. According to our research, it was safety for patients with PRF to sit vertical or recline on the bed during rehabilitation while standing and walking were inappropriate. Our results may bring some theoretical guidance for clinical nursing and treatment in patients with PRF.

Acknowledgments

Footnote

Conflicts of Interest: The authors have no conflicts of interest to declare.

References

1. Langford JR, Burgess AR, Liporace FA, et al. Pelvic Fractures: Part 1. Evaluation, Classification, and Resuscitation. J Am Acad Orthop Surg 2013;21:448-57.
2. Gray A, Chandler H, Sabri O. Pelvic ring injuries: classification and treatment. Orthop Trauma 2018;32:80-90.
3. Blum L, Hake ME, Charles R, et al. Vertical shear pelvic injury: evaluation, management, and fixation strategies. Int Orthop 2018;42:2663-74.
4. Langford JR, Burgess AR, Liporace FA, et al. Pelvic fractures: part 2. Contemporary indications and techniques for definitive surgical management. J Am Acad Orthop Surg 2013;21:458-68.
5. Alvi F, Kumar A, Clayson AD. Open reduction and internal fixation of an unstable pelvic ring injury during pregnancy. Arch Orthop Trauma Surg 2007;8:192-4.
6. Scaglione M, Parchi P, Digrandi G, et al. External fixation in pelvic fractures. Musculoskelet Surg 2010;94:63-70.
7. Schulte FA, Ruffoni D, Lambers FM, et al. Local mechanical stimuli regulate bone formation and resorption in mice at the tissue level. PLoS One 2013;8:e62172.
8. Coppola G, Fortunato DG. Bone mineral density in children, adolescents, and young adults with epilepsy. Epilepsia 2009;50:2140-6.
9. Finbråten AK, Syversen U, Skranes J, et al. Bone mineral density and vitamin D status in ambulatory and non-ambulatory children with cerebral palsy. Osteoporos Int 2015;26:141-50.
10. Susanne C, Claudia G, E Andrea N, et al. Patient risk factors for pressure ulcer development: systematic review. Int J Nurs Stud 2013;50:974-1003.
11. Guo F, Shashikiran T, Chen X, et al. Clinical features and risk factor analysis for lower extremity deep venous thrombosis in Chinese neurosurgical patients. J Neurosci Rural Pract 2015;6:471-6.
12. Brogan E, Langdon C, Brookes K, et al. Respiratory Infections in Acute Stroke: Nasogastric Tubes and Immobility are Stronger Predictors than Dysphagia. Dysphagia 2014;29:340-5.
13. Ifju PG. Composite Materials. Springer Handbook of Experimental Solid Mechanics 2008:97-124.
14. Chung CY. A simplified application (APP) for the parametric design of screw-plate fixation of bone fractures. J Mech Behav Biomed Mater 2018;77:642-8.
15. Li L, Yang L, Yu F, et al. 3D printing individualized heel cup for improving the self-reported pain of plantar fasciitis. J Transl Med 2018;16:167.
16. Li J, Wang M, Li L, et al. Finite element analysis of different configurations of fully threaded cannulated screw in the treatment of unstable femoral neck fractures. J Orthop Surg Res 2018;13:272.
17. Chen WP, Tai CL, Shih CH, et al. Selection of fixation devices in proximal femur rotational osteotomy: clinical complications and finite element analysis. Clin Biomech (Bristol, Avon) 2004;19:255-62.
18. Yamaji T, Ando K, Wolf S, et al. The effect of micromovement on callus formation. J Orthop Sci 2001;6:571-5.
19. Tufekci P, Tavakoli A, Dlaska C, et al. Early mechanical stimulation only permits timely bone healing in sheep. J

Orthop Res 2018;36:1790-6.
20. Claes L, Meyers N, Schulke J, et al. The mode of interfragmentary movement affects bone formation and revascularization after callus distraction. PLoS One

2018;13:e0202702.
21. Frost HM. A 2003 update of bone physiology and Wolff's Law for clinicians. Angle Orthod 2004;74:3-15.

Cite this article as: Li L, Lu J, Yang L, Zhang K, Jin J, Sun G, Wang X, Jiang Q. Stability evaluation of anterior external fixation in patient with unstable pelvic ring fracture: a finite element analysis. Ann Transl Med 2019;7(14):303. doi: 10.21037/atm.2019.05.65